Optical Materials 149 (2024) 115075

Contents lists available at ScienceDirect

Optical Materials

journal homepage: www.elsevier.com/locate/optmat

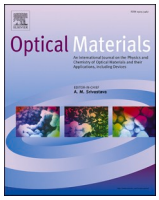

Research Article

Enhancement in photoluminescence from GaPAsN/GaP alloys by 6-MeV electrons irradiation and rapid thermal annealing

E.-M. Pavelescu [a,b,*], D. Ticoş [c], O. Ligor [a], C. Romaniţan [a], A. Matei [a], F. Comănescu [a], V. Ţucureanu [a], S.I. Spânulescu [b], C. Ticoş [d], T. Ohshima [e], T. Nakamura [f], M. Imaizumi [f], R. S. Goldman [g], A. Wakahara [h], K. Yamane [h]

[a] National Institute for Research and Development in Microtechnologies, Erou Iancu Nicolae 126 A, 077190, Voluntari, Romania
[b] Faculty of Exact Sciences and Engineering, Hyperion University, Calea Călăraşilor 169, Bucharest, Romania
[c] National Institute for Laser, Plasma and Radiation Physics, 077125, Bucharest, Romania
[d] ELI-NP, National R&D Institute for Physics and Nuclear Engineering (IFIN_HH), 30 Reactorului Street, 077125, Magurele, Romania
[e] National Institutes for Quantum Science and Technologies, 1233 Watanuki, Takasaki, Gunma, 370-1292, Japan
[f] Japan Aerospace Exploration Agency, 2-1-1 Sengen, Tsukuba, Ibaraki, 305–8505, Japan
[g] Department of Materials Science and Engineering, University of Michigan, Ann Arbor, MI, 48109-2136, USA
[h] Department of Electrical and Electronic Information Engineering, Toyohashi University of Technology, Toyohashi, Aichi, 441-8580, Japan

ARTICLE INFO

Keywords:
Dilute nitride alloys
Photoluminescence
Electron irradiation
Thermal annealing

ABSTRACT

6-MeV electrons irradiation of a nearly lattice-matched P-rich GaPAsN-on-GaP epilayer, grown by molecular beam epitaxy, and subsequent rapid thermal annealing at 650 °C are found to induce much stronger photoluminescence than what is observed for an identical as-grown sample annealed in similar conditions. At the same time, exciton localization at low temperatures decreased and alloys crystallinity improved as seen by power-dependent photoluminescence and Raman spectroscopy, respectively. These irradiation-related phenomena occurred without change in the alloy macroscopic composition as revealed by X-ray diffraction.

1. Introduction

Extensive studies have been conducted on dilute nitride III–V compounds (III–V–N alloys) due to their unique strong band gap bowing with a decrease in their lattice constant when nitrogen atoms are substituted for the group-V in a *dilute* regime. This has led to expectations for their use in a wide variety of optical and electronic device applications on various substrates. For instance, GaP-rich GaPAsN quaternary alloys are essential candidates for light-emitting and light absorbing devices on Si substrates because of their near-lattice matching to Si and widely tunable bandgap range, enabling current matching conditions for successful integration in tandem cellon Si platform [1–3]. However, unintentional nitrogen-related point defects remain critical for the optical quality of III–V-N alloys, independent of growth technique. In the case of GaPAsN alloys, post-growth rapid thermal annealing (RTA) is effective for improving optical properties but it does so at the expense of an undesired increase in the energy band gap [4], especially at elevated temperatures >700 °C, where the effect of annealing on PL enhancement is pronounced. For InGaAsN [5] and GaAsNBi [6] alloys, irradiation with 6–7 MeV electrons prior to RTA has been shown to augment the effect of RTA at 650 °C, thereby minimizing annealing-induced band gap enlargement. It was recently shown that irradiation with 380 keV protons or electrons followed by RTA at 920 °C leads to enhanced characteristics of a GaPAsN-on-Si solar cell [7]. It is interesting to note that the higher momentum of the protons appear to lead to greater improvements in solar cell performance in comparison to that induced by electrons accelerated with the same energy. Taken together, all these previous electron/proton irradiation treatments applied prior to annealing in dilute nitride quaternary alloys suggest an alternative route for enhancing the optical performance of GaPAsN/GaP alloys by employing irradiation with energetic 6 MeV electrons, and, hence, larger momentum than previously used, but at a lower annealing temperature of 650 °C in order to keep at bay the annealing-induced bandgap increase. Another advantage of lower annealing temperatures ≤700 °C is avoiding the deterioration of the tunneling capabilities of the highly doped tunnel junctions of a tandem cell by the possible annealing-induced dopant interdiffusion across the junctions interfaces at elevated annealing temperatures.

* Corresponding author. National Institute for Research and Development in Microtechnologies, Erou Iancu Nicolae 126 A, 077190, Voluntari, Romania
E-mail address: emil.pavelescu@imt.ro (E.-M. Pavelescu).

https://doi.org/10.1016/j.optmat.2024.115075
Received 18 September 2023; Received in revised form 2 February 2024; Accepted 9 February 2024
Available online 21 February 2024

2. Experimental details

The $GaP_{0.765}As_{0.19}N_{0.045}$ wafer investigated in this work was grown at 550 °C on a semi-insulating GaP (0 0 1) substrate using a molecular beam epitaxy (MBE) apparatus (EpiQuest RC2100WT). Following growth, 4 pieces of ~3 mm × 3 mm were cut from the same region of the wafer. After that, two pieces were irradiated with 6 MeV electrons to the 10^{15} electrons/cm^2 fluence. For both as-grown and electron-irradiated pieces, which we term "as-grown" and "e-irradiated" GaPAsN, RTA was performed for 1 min at 650 °C in dry nitrogen. For all samples, high resolution X-ray diffraction (HR-XRD) was performed using a Rigaku diffractometer. The HR-XRD spectra for all quaternary layers reveal (Fig. 1) similar positions and line-widths of the epilayer peaks, independent of electron irradiation and/or RTA, indicating minimal changes in the N mole fraction and overall crystalline quality [8].

For photoluminescence (PL), the samples were mounted inside a closed-cycle He cryostat and photo-excited with the 532 nm line of a YAG:Nd CW laser operating at 100 mW. The luminescence was collected in front surface configuration into a monochromator and detected by a thermoelectrically-cooled InGaAs photodetector. The PL spectra were not corrected by taking into account the spectral sensitivity of the set-up used. Raman measurements were performed in the back scattering geometry at room temperature (RT) using a Horiba Jobin Yvon micro-Raman spectrometer under 632.8 nm excitation.

3. Results and discussion

In Fig. 2 are presented the RT and low temperature (LT) PL spectra of the as-grown and e-irradiated samples before and after the RTA stage. All the PL spectra are broad presenting tails at both short (high) and, especially, long (low) wavelengths (energies) sides. Very small blue-shifts 4–9 nm (10–25 meV) have also been measured for the PL spectra with the decrease in the samples temperature within the investigated (6–300 K) range. The PL shapes appear to be nearly similar for as-grown and both RTA and e-irradiated samples, suggesting that the main radiative channels have not been affected neither by the electrons irradiation, at the energy and fluence used, nor by the employed RTA treatment, performed at only 100 °C higher than the alloy growth temperature to minimize the annealing-induced blueshift, as it has been observed. All these PL observations can be mainly accounted for by considering that the conduction band edge (CBE) states of the investigated P-rich GaPAsN alloy, with a N content slightly larger than 3% and a relatively small amount of As ≈ 20%, are formed as an „amalgamation" of the nitrogen-perturbed states of the host alloy (P-rich GaPAs) and the nitrogen-containing localized (pinned) cluster states, including

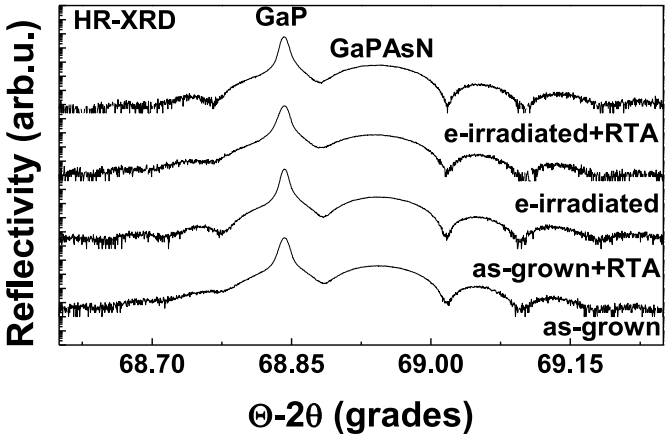

Fig. 1. High-resolution X-rays diffraction (HR-XRD) curves from the as-grown and e-irradiated $GaP_{0.765}As_{0.19}N_{0.045}$/GaP samples recorded before and after rapid thermal annealing (RTA) at 650 °C for 1 min.

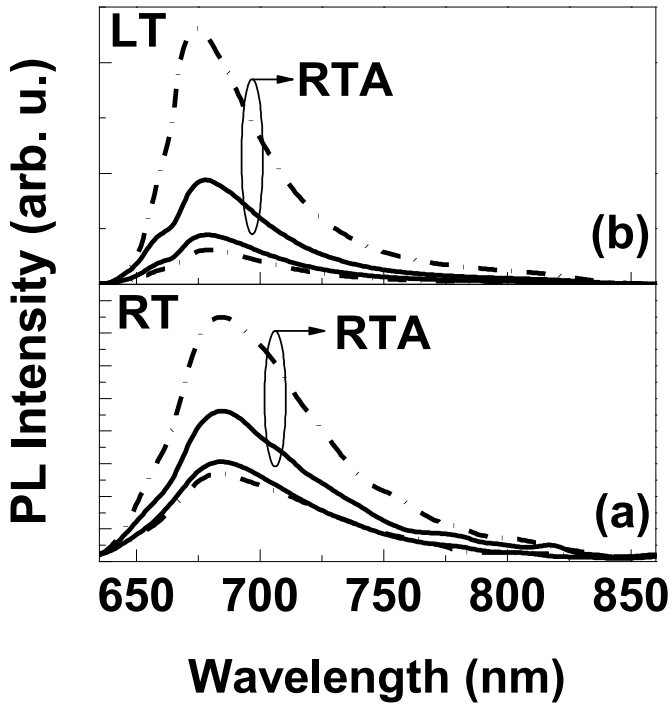

Fig. 2. Photoluminescence (PL) recorded before and after rapid thermal annealing (RTA) from the as-grown (continuous lines) and e-irradiated (dash-dotted lines) at (a) room temperature (RT) and (b) low temperature (LT).

mainly pair, triplet and quadruplet states, appearing inside the bandgap [9]. Thus the alloy emission is broad, composed of several possible radiative recombination channels, having tails on both sides, especially on the long (high) wavelengths (energy) side corresponding to the deepest localized states. The pinned states confer the mixed CBE a strong localization character, explaining the good stability of the emission with temperature variation. The N-containing clusters are thought to be thermally stable at temperatures below 700 °C, explaining in part the negligible change in the PL shape with the RTA at 650 °C. If the PLs shapes and spectral positions are only marginally affected by the e-irradiation and/or RTA, their PL intensities appear instead to be noticeably affected. Thus, PL intensities of the e-irradiated GaPAsN sample is less than that of the corresponding as-grown sample, revealing introduction of non-radiative defects or a change in the properties of the already existing ones by the electrons irradiation [5,6,10]. The only 12% deterioration of RT PL observed in the GaPAsN sample suggests a higher radiation hardness of this alloy compared to the InGaAsN [5] and GaAsNBi [6] ones where large decrease (more than 50 %) in PLs were previously observed after similar exposure with electrons. Despite the initial PL deterioration, the electron irradiation has induced a remarkable enhancement in PL intensity upon annealing. Notably, the PL intensity of the annealed e-irradiated sample became more than 1.6 and 2.4 more intense at RT and LTs, respectively, than that of their corresponding annealed as-grown sample, indicating that the electron irradiation promotes a more efficient removal of the non-radiative defects upon annealing. This PL enhancement upon annealing promoted by electron irradiation in our $GaP_{0.765}As_{0.19}N_{0.045}$ material and in previously investigated GaInNAs [5] and GaAsBiN [6] alloys suggest that electrons irradiation followed by RTA is a useful technique for healing the poor optical quality of other (quina)quaternary members of dilute nitrides family such as (In)GaAsNSb, especially at higher N contents ≥5 % necessary to get a lower 0.8 eV bandgap and below [11]. One can also notice, this irradiation-promoted PL intensity enhancement occurred at RT without a spectral shift, whereas only 4 nm blue shift was seen at LT upon annealing between the e-irradiated and as-grown samples.

Fig. 3 shows the variation of the peak intensity I(T) of the PL with

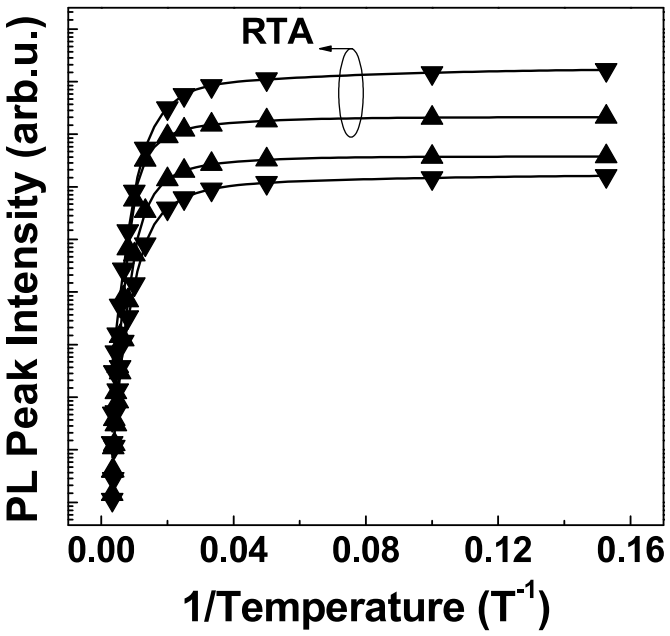

Fig. 3. Arrhenius plots of photoluminescence (PL) peak intensity from the as-grown (up-pointing triangles) and e-irradiated (down-pointing triangles) measured before and after rapid thermal annealing (RTA). The solid curves are the best fits of Eq. (1) to the experimental points, yielding the activation energies E_1, E_2 and E_3 together with the prefactors c_1, c_2 and c_3 given in Table 1.

inverse of absolute temperature 1/T from the as-grown and e-irradiated GaPAsN samples before and upon annealing. The I(T) values can be very well described by the following expression $I(T) = I(0)/[1+c_1\exp(-E_1/k_BT) + c_2\exp(-E_2/k_BT) + c_3\exp(-E_3/k_BT)]$ (1), which can be interpreted in terms of three thermally activated loss (non-radiative) processes with the activation energies E_1,E_2 and E_3, with the prefactors c_1,c_2 and c_3 measuring the efficiency of the corresponding loss mechanisms 1, 2 and 3, respectively [6,12]. We ascribe the observed three loss processes to thermally activated transfers of carriers to nonradiative recombination centres, in this image the prefactors c_i, i = 1,3, being related to the density of the nonradiative centres i. In Table 1 we give E_1, E_2, E_3, c_1, c_2 and c_3 as the best fits to the experimental I(T). The E_1, E_2 and E_3 are not much affected by annealing as well as irradiation and annealing, indicating that the same processes take place in both the as-grown and e-irradiated samples. The low-T and intermediate-T prefactors c_1 and c_2 are also somewhat less influenced by annealing with or without the prior irradiation step. Instead, the high-T prefactor c_3 is clearly smaller for the annealed e-irradiated sample compared to the only annealed one, indicating a reduction of the high-temperature loss mechanism for PL, beneficial for the alloys use in devices operating at higher temperatures. The low and intermediate temperatures loss (non-radiative) channels

Table 1
Activation energies and prefactors obtained by the best fit of Eq. (1) to the experimental photoluminescence intensities as a function of inverse temperature.

Samples	E_1 (meV)	c_1 (arb. u.)	E_2 (meV)	c_2 (arb. u.)	E_3 (meV)	c_3 (arb. u.)
as-grown GaPAsN	4.5 ± 0.3	0.9 ± 0.2	19.4 ± 0.8	22.9 ± 2.6	61.3 ± 7.2	2992.6 ± 124.1
e-irradiated GaPAsN	5.1 ± 0.6	1.5 ± 0.1	20.1 ± 3.4	33.7 ± 3.6	62.1 ± 5.4	3521.4 ± 150.4
as-grown + RTA GaPAsN	4.4 ± 0.4	0.7 ± 0.3	19.8 ± 4.1	12.7 ± 0.9	60.2 ± 4.5	2212.7 ± 166.3
e-irradiated + RTA GaPAsN	5.4 ± 0.5	0.6 ± 0.2	19.1 ± 2.6	11.9 ± 1.7	58.8 ± 5.1	1661.4 ± 142.7

are likely related to carriers trapping at the N-induced localized states and/or alloy disorder caused by N incorporation fluctuations [13] As for the high-T loss mechanism with the averaged E_3 of 61 ± 7 meV, it could be one of the three holes traps with activation energies in the 0.06–0.07 eV range found by DLTS in as-grown and annealed GaPAsN alloys, synthesized by MBE [14]. It could also be ascribed to the non-radiative PL loss mechanism with around 50 meV, derived, as in our case, from the dependence of PL intensity versus temperature in MBE-grown P-rich GaPAsN alloys [15].

In Fig. 4 are presented LT PL spectra collected upon annealing at different excitation powers ranging from 100 mW down to 100 μW and 10 μW for the as-grown and e-irradiated samples, respectively, the luminescence efficiency improvement of the irradiated sample compared to the as-grown one allowing the PL signal acquisition at one magnitude lower excitation power. The PL systematically blue shifted [16] as the excitation power increased and this is associated with excitons localization which usually occurs in dilute nitrides alloys due to energy potential fluctuations, mainly created by the presence of nitrogen. This fluctuating potential creates a tail of the density of states (DOS), mainly at the conduction band edges, which traps excitons at very low temperatures before they recombine. The value of the PL shift with excitation power is lower in the e-irradiated sample (4 nm) with respect to the as-grown one (6 nm), despite it was evaluated over one decade larger range. This suggests that the magnitude of potential

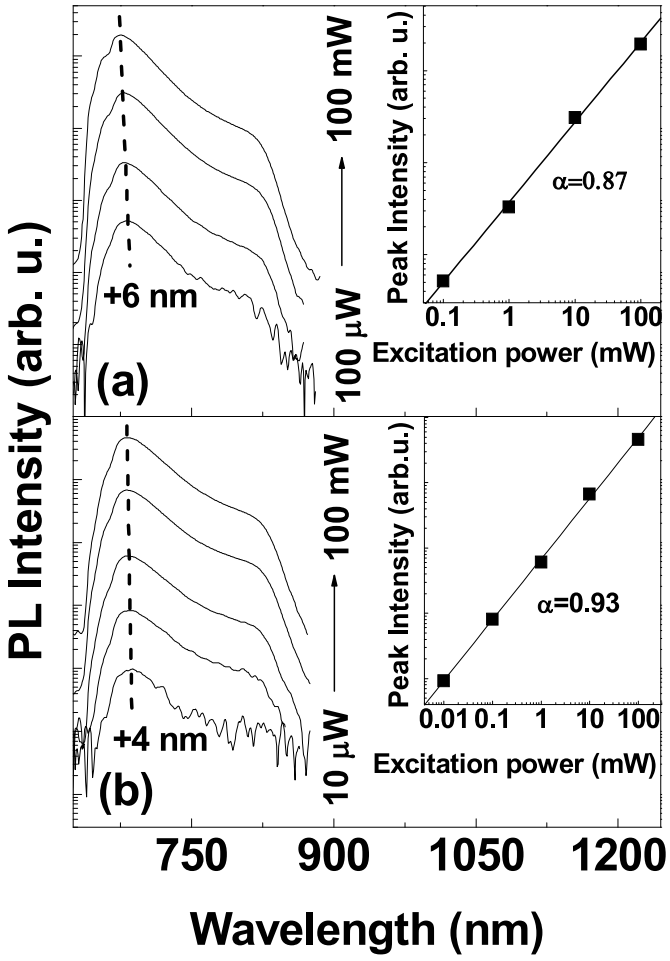

Fig. 4. Excitation power dependence of photoluminescence (PL) spectra collected after rapid thermal annealing (RTA) from (a) as-grown and (b) e-irradiated samples. The dashed lines through the PL peak intensities are drawn to guide an eye. In the insets are shown the dependence of peak intensity versus the excitation power of PLs in logarithmic scale. Also shown are the linear fits (continuous lines) to the experimental data and their slopes (α).

fluctuations, and, hence, their capability of trapping excitons at low temperatures, reduced upon annealing in the e-irradiated GaPAsN alloy compared to the as-grown one. In other words, irradiation helped remove effectively potential energy fluctuations upon annealing. The e-irradiation-promoted decrease in the localization of low-temperature PL excitons is also supported by the plot in logarithmic scale of the PL peak intensity (I) versus excitation power (P) for the two annealed samples, shown in the insets of Fig. 4(a) and (b). The experimental points were very well fit with a linear function whose slope $\alpha = d(\log I)/d(\log P)$ was found 0.87 and 0.93 for the annealed as-grown and e-irradiated samples, respectively. Not shown here, α slopes of 0.82 and 0.81 were measured before RTA in the 100 μW - 100 mW range from the as-grown and e-irradiated samples, respectively, suggesting that the irradiation did not affect the dynamics of PL at low temperatures. The subunity α values at low temperatures seen in our dilute nitride material is indicative of excitons localization, as previously observed in quaternary GaInNAs alloys [16], where α around 0.7 were extracted from excitation power dependent PL at 10 K and linked to the existence of N-related alloys potential fluctuations. The increase in the α slopes upon RTA to values approaching 1, which is in theory expected for free excitons [17] points towards a reduction of degree of excitons localization and, hence, towards a decrease of the alloy potential fluctuations. Noticeably, the larger irradiation-promoted enhancement of the α value approaching 1 encountered upon RTA in the e-irradiated sample compared to the as-grown one suggests an irradiation-promoted more efficient decrease of the alloy potential fluctuations upon RTA. This translates into a more effective reduction of the bandgap energy tail, decreasing thus its capability of trapping excitons at low temperatures. This could explain the small PL blue shift upon annealing observed at low temperatures only in the e-irradiated sample [18].

Fig. 5 shows Raman scattering spectra in the 345-415 cm^{-1} range of the as-grown and e-irradiated GaPAsN before and after annealing. The curves are dominated by a strong GaP-like longitudinal-optic (LO) mode, labeled LO_1, and a weaker transverse-optic (TO) mode, labeled TO_1. The spectra contain an additional band, labeled X, situated at around 386 cm^{-1}. This mode was previously reported in Raman spectra of GaAsP alloys [19,20] and also observed in GaPN layers [21] or in the shell of the GaP/GaPN nanowires (NWs) [22]. Its energy is very close to

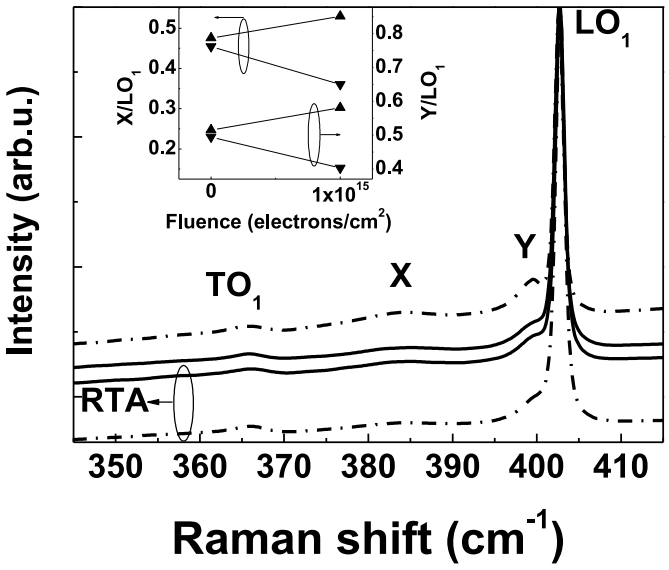

Fig. 5. Raman spectra of the as-grown (continuous lines) and e-irradiated (dash-dotted lines) GaPAsN/GaP samples normalized to the intensity of the LO_1 band taken before and after rapid thermal annealing (RTA) using the 632.8 nm laser line. In the inset are shown the ratios of the peak intensities of X and Y bands with respect to the intensity of LO_1 band measured before (up-pointing triangles) and after (down-pointing triangles) the RTA.

the LO phonon energy at the X-point of the Brillouin zone of GaP. Even though the exact origin of this mode is not known, its appearance in the disordered GaP-based alloys implies that it is likely activated by the compositional disorder, which can be further enhanced or induced by nitrogen incorporation. This alloy inhomogeneity leads to activation of this forbidden mode by the relaxation of the momentum conservation rules by breaking the translational symmetry. At the low-energy side of the LO_1 mode, one can also notice another additional Raman feature, labeled Y. For the as-grown and annealed samples, this feature embraces the form of a shoulder on the left side of the LO_1 mode but then it evolves as a distinctive peak at 399 cm^{-1} after the electron irradiation of the as-grown sample. Little is also known about the nature of this Raman feature, a mode at 397 cm^{-1} being previously found in GaN/GaPN NWs and tentatively attributed to resonant Raman scattering via defect states located in the vicinity of the NW surfaces [22]. The enhancement of this mode upon electrons irradiation, which generates new point defects or affects the existing ones, also hints towards the involvement of defects, whose localization might be close to the quaternary alloy surface. As shown in the inset of Fig. 5, the relative intensities of the additional Raman modes X and Y compared to the intensity of the dominant LO_1 mode increase upon electron irradiation and then decrease after thermal annealing and it does so more for the irradiated sample compared to the non irradiated one, suggesting an electron irradiation-promoted diminution on annealing of the mechanisms generating these modes, whose presence in the Raman spectrum are tentatively associated with alloy imperfections. As for the origin of the X and Y bands, it is worth mentioning that none of the bands was observed in the Raman spectrum of the GaP substrate used to grow the quaternary alloy. Instead, the X Raman band appeared whereas the Y band remained still absent in a GaPN/GaP sample with less 2.2% N grown in similar conditions as the investigated GaPAsN sample. These indicate that the X band is mainly connected with the presence of N into GaP whereas the appearance of the Y band involves the additional As incorporation into the GaPN alloy.

It has been shown that a large amount of nitrogen incorporates into off-substitutional sites in MOCVD-grown GaPN, especially at larger nitrogen concentrations ≈4%, generating point defects, such as nitrogen interstitials, vacancies and nitrogen defect complexes composed of multiple nitrogen atoms [23]. This scenario is expected to also occur when growing P-rich GaPAsN alloys with large N contents >4 % by MBE, taking additionally into account that the growth of GaPAsN is accomplished in MBE at much lower temperatures than normally used to synthetize it by MOCVD. These N-related defects could act as non-radiative and/or scattering centres for carriers, explaining the drastic decrease in luminescence efficiency and broadening of the emission linewidth usually seen not only in GaPAsN but also in all dilute nitrides alloys compared to their N-free parent matrixes. At the same time, these N-containing defects, notably, N–P and N–N pairs at the group V site [24], $(N–P)_V$ and $(N–N)_V$, respectively, generating localized cluster states and compositional disorder, lead to potential fluctuations of the alloy energy bands edges and/or local distortions of the GaPAsN lattice reflected in considerable localization of excitons at low temperatures and the appearance of otherwise forbidden Raman bands. Thus, the removal and/or structural transformation upon annealing of these N-containing point defects leads to an enhancement in PL, by eliminating their associated deep levels [9], and an improvement in crystallinity, without a noticeable change in the alloy composition.

The previously observed PL enhancement in quaternary GaAsNBi [6] alloys after 6-MeV electrons irradiation followed by RTA, clearly linked to the nitrogen presence in the alloys, and the recently seen N-related improvement in P-rich GaPAsN solar cell performance after 0.3 MeV proton irradiation followed by RTA [7] suggest that the found PL intensity improvement in our 6-MeV-electrons-irradiated GaPAsN alloy upon annealing is also linked to its native N-related nonradiative defects. The way this irradiation-promoted efficient removal on annealing of the N-linked defects occurs is most likely by a vacancy mediated mechanism of annihilation on annealing of these defects, as previously

shown in the 0.3 MeV proton-irradiated P-rich GaPAsN solar cells [24], knowing the 6-MeV electrons also creates vacancies throughout the entire GaPAsN layer according to the Stopping and Range of Ions in Matter formalism [25].

4. Conclusions

In summary, irradiation with 6 MeV electrons to the fluence of 10^{15} electrons/cm^2 was found to deteriorate the photoluminescence of a $GaP_{0.765}As_{0.19}N_{0.045}$ epilayer grown on GaP by molecular beam epitaxy. When rapid thermally annealed at 650 °C for 1 min a remarkable enhancement in PL intensity was resulted in which was much larger than the enhancement in intensity seen in the corresponding as-grown sample annealed in the same conditions. At the same time, the degree of excitons localization at low temperatures decreased, suggesting a reduction of the alloy potential fluctuations, and the alloy crystallinity improved, as inferred from the Raman spectroscopy. The observed irradiation-induces changes in PL upon thermal treatment occurred without change in the alloy macroscopic composition, as revealed by X-ray diffraction measurements.

CRediT authorship contribution statement

E.-M. Pavelescu: Conceptualization, Formal analysis, Funding acquisition, Investigation, Validation, Writing – original draft, Writing – review & editing. **D. Ticoş:** Formal analysis, Validation, Writing – review & editing. **O. Ligor:** Formal analysis, Investigation, Validation, Writing – review & editing. **C. Romaniţan:** Validation, Writing – review & editing. **A. Matei:** Formal analysis, Validation. **F. Comănescu:** Validation. **V. Ţucureanu:** Investigation, Validation. **S.I. Spânulescu:** Validation, Writing – review & editing. **C. Ticoş:** Funding acquisition, Validation, Writing – review & editing. **T. Ohshima:** Validation. **T. Nakamura:** Validation. **M. Imaizumi:** Validation, Writing – review & editing. **R.S. Goldman:** Validation, Writing – review & editing, Writing – original draft. **A. Wakahara:** Supervision, Validation, Writing – original draft. **K. Yamane:** Conceptualization, Validation, Writing – original draft, Writing – review & editing.

Declaration of competing interest

The authors declare that they have no known competing financial interests or personal relationships that could have appeared to influence the work reported in this paper.

Data availability

Data will be made available on request.

Acknowledgement

This work was supported by a grant of the Ministry of Research, Innovation and Digitization, CCCDI-UEFISCDI, project number PN-III-P2-2.1-PED-2021-3525, within PNCDI III.

References

[1] K. Yamane, K. Noguchi, S. Tanaka, Y. Furukawa, H. Okada, H. Yonezu, A. Wakahara, Operation of monolithically-integrated digital circuits with light emitting diodes fabricated in lattice-matched Si/III–V–N/Si heterostructure, Appl. Phys. Express 3 (2010) 074201, https://doi.org/10.1143/APEX.3.074201.

[2] K. Zelazna, M. Gladysiewicz, M.P. Polak, et al., Nitrogen-related intermediate band in P-rich $GaN_xP_yAs_{1-x-y}$ alloys, Sci. Rep. 7 (2017) 15703, https://doi.org/10.1038/s41598-017-15933-1.

[3] R. Kudrawiec, A.V. Luce, M. Gladysiewicz, M. Ting, Y.J. Kuang, C.W. Tu, O. D. Dubon, K.M. Yu, W. Walukiewicz, Electronic band structure of GaNxPyAs1−x−y highly mismatched alloys: suitability for intermediate-band solar cells, Phys. Rev. Appl. 1 (2014) 034007, https://doi.org/10.1103/PhysRevApplied.1.034007.

[4] K. Yamane, K. Sato, H. Sekiguchi, H. Okada, A. Wakahara, Doping control of GaAsPN alloys by molecular beam epitaxy for monolithic III-V/Si tandem solar cells, J. Cryst. Growth 473 (2017) 55–59, https://doi.org/10.1016/j.jcrysgro.2017.05.025.

[5] E.M. Pavelescu, R. Kudrawiec, N. Baltateanu, S. Spânulescu, M. Dumitrescu, M. Guina, Enhancement in photoluminescence from 1 eV GaInNAs epilayers subject to 7 MeV electron irradiation, Semicond. Sci. Technol. 28 (2013) 025020, https://doi.org/10.1088/0268-1242/28/2/025020.

[6] E.M. Pavelescu, O. Ligor, J. Occena, C. Ticos, A. Matei, R.L. Gavrila, K. Yamane, A. Wakahara, R.S. Goldman, Influence of electron irradiation and rapid thermal annealing on photoluminescence from GaAsNBi alloys, Appl. Phys. Lett. 117 (2020) 142106, https://doi.org/10.1063/5.0027400.

[7] K. Yamane, R. Futamura, S. Genjo, D. Hamamoto, Y. Maki, E.-M. Pavelescu, T. Ohsima, T. Sumita, M. Imaizumi, A. Wakahara, Improved crystallinity of GaP-based dilute nitride alloys by proton/electron irradiation and rapid thermal annealing, Jpn. J. Appl. Phys. 61 (2022) 020907, https://doi.org/10.35848/1347-4065/ac4a06.

[8] K.C. Dimiduk, C.Q. Ness, J.K. Foley, Electron irradiation of GaAsP LEDS, IEEE Trans. Nucl. Sci. 32 (1985) 4010, https://doi.org/10.1109/TNS.1985.4334060.

[9] P.R.C. Kent, A. Zunger, Theory of electronic structure evolution in GaAsN and GaPN alloy, Phys. Rev. B 64 (2001) 115208, https://doi.org/10.1103/PhysRevB.64.115208.

[10] S.G. Cherkova, et al., Formation of light-emitting defects in silicon by swift heavy ion irradiation and subsequent annealing, Nucl. Instrum. Methods Phys. Res. B 535 (2023) 132–136, https://doi.org/10.1016/j.nimb.2022.12.00411.

[11] R. Isoaho, A. Aho, A. Tukiainen, T. Aho, M. Raappana, T. Salminen, J. Reuna, M. Guina, Photovoltaic properties of low-bandgap (0.7–0.9 eV) lattice-matched GaInNAsSb solar junctions grown by molecular beam epitaxy on GaAs, Sol. Energy Mater. Sol. Cells 195 (2019) 198, https://doi.org/10.1016/j.solmat.2019.02.030.

[12] S.G. Cherkova, V.A. Volodin, F. Zhang, M. Stoffel, H. Rinnert, M. Vergnat, Optical properties of GeO[SiO] and GeO[SiO_2] solid alloy layers grown at low temperature, Opt. Mater. 122 (2021) 111736, https://doi.org/10.1016/j.optmat.2021.111736.

[13] H.A. Alburaih, H. Albalawi, M. Henini, Investigation of the effect of different thicknesses and thermal annealing on the optical properties of GaAsPN alloys grown on GaP substrates, Mater. Sci. Semicond. Process. 117 (2020) 105143, https://doi.org/10.1016/j.mssp.2020.105143.

[14] H.A. Alburaih, H. Albalawi, M. Henini, Effect of rapid thermal annealing on the electrical properties of dilute GaAsPN based diodes, Semicond. Sci. Technol. 34 (2019) 105009, https://doi.org/10.1088/1361-6641/ab3671.

[15] M. Wełna, K. Zelazna, A. Letoublon, C. Cornet, Ł. Janicki, M.S. Zielinski, R. Kudrawiec, Radiative and nonradiative recombination processes in GaNP(As) alloys, Mater. Sci. Eng. B 276 (2022) 115567, https://doi.org/10.1016/j.mseb.2021.115567.

[16] E.-M. Pavelescu, T. Jouhti, C.S. Peng, W. Li, J. Konttinen, M. Dumitrescu, P. Laukkanen, M. Pessa, Enhanced optical performances of strain-compensated 1.3-mm GaInNAs/GaNAs/GaAs quantum-well structures, J. Cryst. Growth 241 (2002) 31, https://doi.org/10.1016/S0022-0248(02)01133-8.

[17] T. Schmidt, K. Lischka, W. Zulehner, Excitation-power dependence of the near-band edge photoluminescence of semiconductors, Phys. Rev. B 16 (1992) 8989, https://doi.org/10.1103/PhysRevB.45.8989.

[18] M. Yoshimoto, W. Huang, Y. Takehara, J. Saraie, A. Chayahara, Y. Horino, K. Oe, New semiconductor GaNAsBi alloy grown by molecular beam epitaxy, Jpn. J. Appl. Phys. 43 (2004) L845, https://doi.org/10.1143/JJAP.43.L845.

[19] D. Schmeltzer, R. Beserman, Localized states in mixed GaP_zAs_{1-z} crystals, Phys. Rev. B 22 (1980) 6330, https://doi.org/10.1103/PhysRevB.22.6330.

[20] C. Ramkumar, K.P. Jain, S.C. Abbi, Resonant Raman scattering probe of alloying effect in $GaAs_{1-x}P_x$ ternary alloy semiconductors, Phys. Rev. B 54 (1996) 7921, https://doi.org/10.1103/physrevb.54.7921.

[21] I.A. Buyanova, W.M. Chen, E.M. Goldys, H.P. Xin, C.W. Tu, Structural properties of a GaN_xP_{1-x} alloy: Raman studies, Appl. Phys. Lett. 78 (2001) 3959, https://doi.org/10.1063/1.1380244.

[22] A. Drobovolski, S. Sukrittanon, Y.J. Kuang, C.W. Tu, W.M. Chen, I.A. Buyanova, Energy upconversion in GaP/GaNP core/shell nanowires for enhanced near-infrared light harvesting, Appl. Phys. Lett. 105 (2014) 193102, https://doi.org/10.1002/smll.201401342.

[23] H. Jussila, K.M. Yu, J. Kujala, F. Tuomisto, S. Nagarajan, J. Lemettinen, T. Huhtio, T.O. Tuomi, H. Lipsanen, M. Sopanen, Substitutionality of nitrogen atoms and formation of nitrogen complexes and point defects in GaPN alloys, J. Phys. D Appl. Phys. 47 (2014) 075106, https://doi.org/10.1088/0022-3727/47/7/075106.

[24] K. Yamane, Y. Maki, S. One, A. Wakahara, E.-M. Pavelescu, T. Ohshima, T. Nakamura, M. Imaizumi, Mechanism of improved crystallinity by defect-modification in proton-irradiated GaAsPN photovoltaics: experimental and first-principle calculations approach, J. Appl. Phys. 132 (2022) 065701, https://doi.org/10.1063/5.0096345.

[25] J.F. Ziegler, M.D. Ziegler, J.P. Biersack, SRIM – The stopping and range of ions in matter, Nucl. Instrum. Methods Phys. Res. B 268 (2010) 1818, https://doi.org/10.1016/j.nimb.2010.02.091.